The Self-Destructing Internal Gravity Wave

WALTER L. JONES

National Center for Atmospheric Research,[1] Boulder, Colo. 80302

AND DAVID D. HOUGHTON[2]

Dept. of Meteorology, University of Wisconsin, Madison 53706

(Manuscript received 28 February 1972)

ABSTRACT

A simple numerical model is used to demonstrate that momentum exchange between wave and mean flow can substantially modify the process of "breaking" of internal gravity waves at great height. The momentum exchange results in appreciable transfer of energy from wave to mean flow.

1. Introduction

An internal gravity wave propagating upward in the atmosphere grows in amplitude with height, a result of the decreasing atmospheric density. It has long been recognized that the linearized equations used in wave theory must break down at some height. Acoustic waves, which share this problem, should in theory form shock waves (Einaudi, 1969). However, the dispersive nature of internal gravity waves and their essentially transverse rather than longitudinal wave character at low frequencies rule out a simple extension of acoustic theory.

Several authors (Hines, 1963; Hodges, 1967; Lindzen, 1968; Orlanski and Bryan, 1969) have proposed that when internal gravity waves reach a certain amplitude, they produce local conditions of either convective or shear instability. The growth of turbulence in such regions would then draw energy from the wave.

This theory has been developed simply by superimposing the wind and either the density or the potential temperature gradients of the linearized wave on an unperturbed background and looking for Richardson numbers that are less than $\frac{1}{4}$ or negative. This neglects any nonlinear self-interaction of the wave and any interaction between the wave and the background state. The rationale for this neglect has been that in a periodic, progressive, low-frequency internal gravity wave, the perturbation motions occur largely at right angles to perturbation gradients; advective nonlinear terms then remain small. One must note, however, that this idealization does not hold for transients nor for combinations of more than one mode, such as standing waves.

It has also been recognized (cf. Bretherton, 1969a, b; Lindzen and Holton, 1968; Jones and Houghton, 1971) that waves transport momentum and can produce significant changes in the "mean" state of the atmosphere. In the case of rotating and buoyant media, the full description of the wave momentum flux is not straightforward (Bretherton, 1969a; Jones, 1971), but if we neglect rotation, the vertical flux of horizontal momentum is given by the Reynolds stress of the wave.

In a steady periodic wave solution, this momentum flux is constant with height, and thus there is no gradient of Reynolds stress acting on the mean flow. If one considers a wave packet, there are gradients of the Reynolds stress at the front and back of the packet. As the packet passes over a point, a change in mean flow is produced and then cancelled out by the gradients at the packet tail. If the packet is dissipated, a residual momentum is left in the mean flow.

In these cases, the change of mean flow is of second order and is of no consequence if the wave is of small amplitude. Large waves may significantly modify the background in which they propagate. Matsuno (1971) has recently investigated the mean flow interaction of Rossby wave modes propagating vertically and shown that such waves can produce dramatic changes in mean flow, creating critical layers which then stop the upward wave propagation. Matsuno associates these changes with the sudden midwinter warmings in the polar stratosphere and mesophere.

Our objective has been to demonstrate numerically that internal gravity waves can interact so strongly with the mean flow as to modify the "breaking" processes that result from formation of instabilities.

The numerical model we have used is described elsewhere (Houghton and Jones, 1969; Jones and Houghton, 1971) and will not be given in detail here. The model

[1] The National Center for Atmospheric Research is sponsored by the National Science Foundation.

[2] Research supported by the Atmospheric Sciences Section, National Science Foundation, under NSF Grant-12112.

describes in terms of time and vertical position the behavior of linearized gravity and acoustic waves in a planar nonrotating atmosphere. Periodic behavior with one wavenumber is assumed in the horizontal. The wave is coupled dynamically to the mean flow through divergence of the Reynolds stress and through terms involving the mean flow that appear in the wave equations.

Above a height of 100 km, an artificial Rayleigh damping is applied with exponentially increasing strength to prevent reflection of waves at the model top, i.e., to provide a radiation boundary condition. Thus, the behavior above 100 km is not "physical" and should be disregarded.

A true viscosity, simulating crudely the effects of eddy viscosity, has also been added to the model (Appendix). This provides a wavelength-dependent dissipation for waves below 100 km.

Waves are generated at the bottom of the model by, in effect, dragging a corrugated bottom in the horizontal direction. In these studies, we have assumed a horizontal wavelength of 15 km.

Quantities as functions of height are shown in Figs. 1 and 2 for several times. The first quantity is a density-weighted perturbation horizontal velocity, the product of wave horizontal velocity and the square root of mean density. The density weighting is necessary to keep the output on scale; the wave perturbation amplitude varies by factors of hundreds over the 100-km height range. The square of the amplitude of the weighted perturbation velocity is the wave horizontal kinetic energy density and is, therefore, a rough guide to total wave energy density.

The second quantity shown is the mean flow velocity. This is initially set to zero at all heights, and changes are introduced by interaction with the waves. One should note that a given amount of momentum added to the mean flow produces much greater changes in mean flow velocity at greater heights with lower density. Thus, a wave packet may produce similar order-of-magnitude changes in mean flow momentum at all heights, but these effects will be visible as velocity changes only in the upper part of the model.

We shall present results from two numerical experiments. In the first case, four cycles of a wave of 10-min period are forced at the model bottom. In the second case, a continuous random forcing is applied to generate a spectrum of waves with various frequencies but with the same horizontal wavelength, 15 km. Wave amplitude depends on the amplitude of vertical velocities forced at the lower boundary. In the first case, horizontal perturbation velocities are about 40 cm sec^{-1} at the ground. Forcing amplitudes are comparable in the second case; as wave modes of small vertical group velocity are generated, there is an accumulation of wave energy at low altitude over the course of the run.

2. The wave packet

Figs. 1a–d show the evolution of the wave packet and mean flow at several times. In Fig. 1a, the packet is well defined but the momentum changes in mean flow have occurred at dense levels of the atmosphere and are not visible.

Actually, a packet of limited length such as this is not truly monochromatic; such a packet has a frequency spectrum with a major peak at the driving frequency and secondary peaks at n/m times the driving frequency, where m is the number of cycles in the packet forcing and n takes integral values. Some of the higher frequency components of the "packet" move upward with greater group velocity; this effect shows up in Fig. 1a as longer wavelengths associated with the wave at greater heights.

By 1.8 (Fig. 1b), some of the transient precourser to the packet have reached 80–100 km and have produced many tens of meters per second change in mean flow velocity. (The reader should keep in mind that Rayleigh damping has suppressed both wave and mean flow change above 100 km).

At 2.5 hr (Fig. 1c), a broad nose in the mean wind profile has developed. There is also a marked change in the character of the packet; its wavelength has decreased markedly. This is the result of a critical level for the wave that has been established in the mean flow by the leading portion of the packet (Booker and Bretherton, 1967).

The wave we have generated moves in the negative horizontal direction with a horizontal trace velocity of 25 m sec^{-1}. In the process of accelerating the mean flow, there is Doppler shifting of the wave frequency relative to the ground, so that frequencies in the packet are higher than originally generated and critical levels will be at higher negative mean flow velocities. Since there is a spread in frequencies in the packet, there is a corresponding spread in critical levels.

A wave packet approaching a critical level undergoes a shortening of vertical wavelength. This change enhances the tendency to produce instability since both wind shear and density or potential temperature gradients are increased. At the same time, dissipative effects are also increased. In effect, there is a race between dissipation and instability in a packet approaching a critical layer, with the results being influenced by the amplitude of the wave. In this case, the wave has created its own critical level and its amplitude is more or less predetermined.

Unfortunately, this model with its very limited horizontal resolution cannot accurately describe the growth of instabilities. Instead, we have computed the maximum local Richardson numbers as functions of height and time. Richardson numbers exceed $\frac{1}{4}$ for the main body of the wave packet for runs with eddy viscosity of 100 m^2 sec^{-1}, 20 m^2 sec^{-1}, and with only the inherent damping of the model with no explicit viscosity.

Negative Richardson numbers are obtained in the more chaotic precourser region above the main packet, above 75 km in Fig. 1c. The much more irregular nature of mean flow and wave may reflect the efforts of the model to produce instabilities.

The bulk of the packet dissipates smoothly as seen in Fig. 1d. This occurs less rapidly with the lower values of eddy viscosity.

The nose that has developed in the mean wind profile represents a considerable increase in mean flow kinetic energy. We have compared this increase with the amount of work done at the model bottom in generating the disturbance, the wave pressure vertical velocity correlation. With a viscosity of 100 m^2 sec^{-1}, about 27% of the energy supplied ends up in the mean flow. With a viscosity of 20 m^2 sec^{-1}, 38% of the energy shows up in the mean flow.

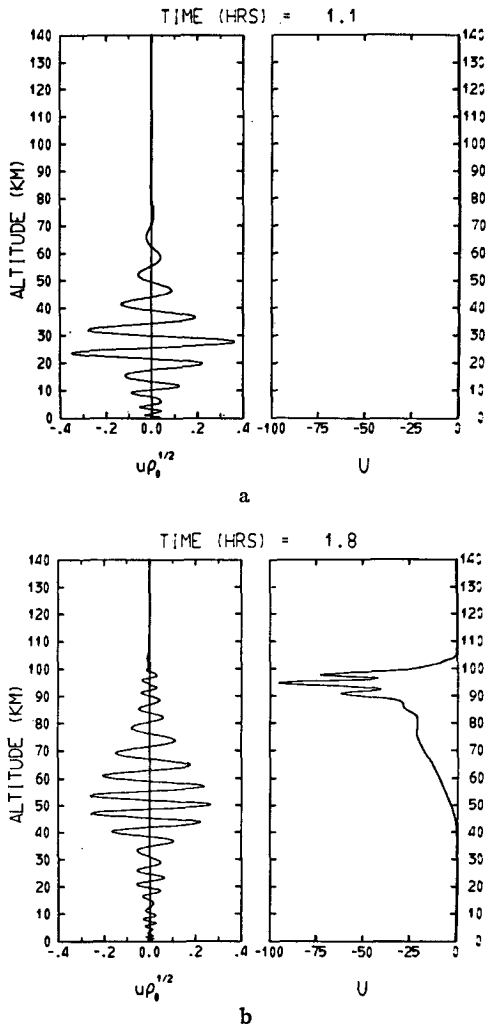

FIG. 1. Horizontal wave velocity weighted by the square root of density $u\rho_0^{\frac{1}{2}}$ and mean flow velocity U as functions of height at: a) 1.1, b) 1.8, c) 2.5, and d) 3.2 hr after initiation of forcing. Four cycles of a 10-min period, 15-km wavelength wave are generated at the ground. Velocities are in m sec^{-1} and density is taken as unity at the ground. Sound speed is 300 m sec^{-1}, gravitational acceleration is 9.8 m sec^{-2}, and viscosity is 100 m^2 sec^{-1}. Artificial damping is employed above 100 km.

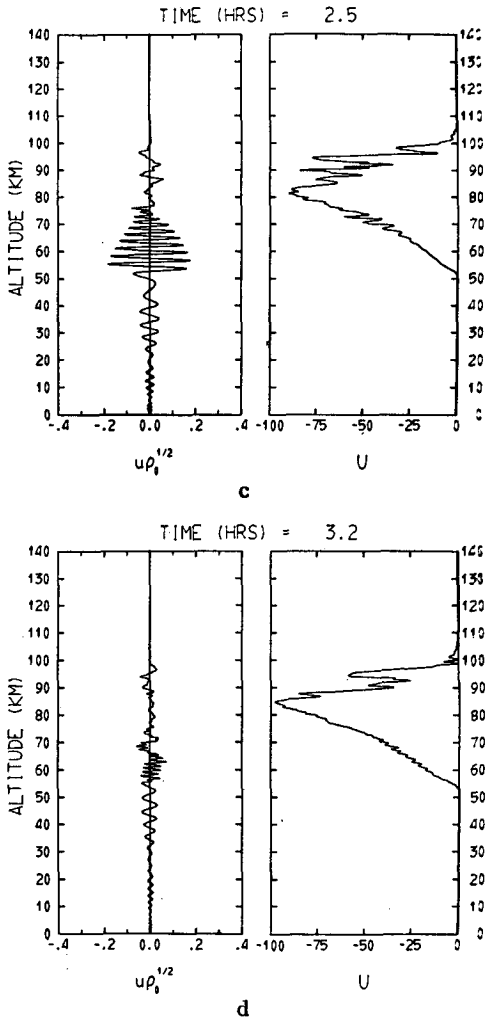

FIG. 1. (*continued*).

3. Random forcing

Fig. 2 presents results from a run in which a random set of waves moving in both directions is generated. The horizontal wavelength and vertical velocity amplitude at the bottom were held constant, while the vertical velocity phase received a small random positive or negative increment at each time step.

The resultant wave spectrum included both acoustic and internal gravity wave modes. The acoustic modes were clearly discernible in 16-mm movie output since they showed upward phase propagation and high frequency, whereas internal gravity modes showed downward phase progression and low frequency.

In Fig. 2a, the disturbances below 60 km are predominantly internal gravity waves. Waves of short

vertical wavelength have small vertical components of group velocity and are more concentrated at lower levels throughout the run. Acoustic modes have had time to reach high levels, but they are not efficient transporters of momentum and have produced only small changes in high-level mean flow.

In Fig. 2b, the fastest internal gravity wave modes have reached the upper atmosphere and produced wind noses of both signs. A positive wind nose serves as a critical layer trap for waves moving with positive horizontal trace velocities; such modes feed more momentum into the mean wind nose. Waves with negative horizontal trace velocities are transmitted (or possibly reflected) by a positive mean wind nose. Of course, the inverse holds for negative wind noses.

Further development of the mean wind profile is shown in Figs. 2c and 2d. Additional noses are developed

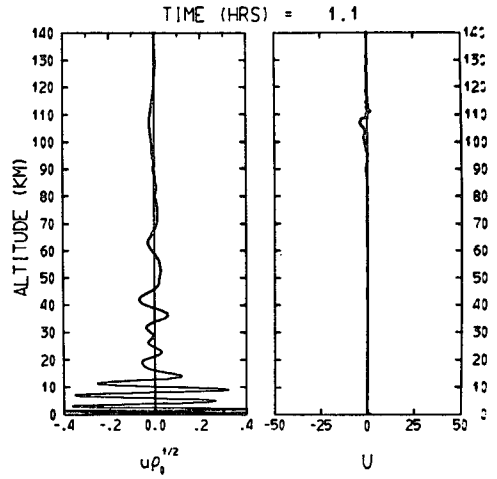

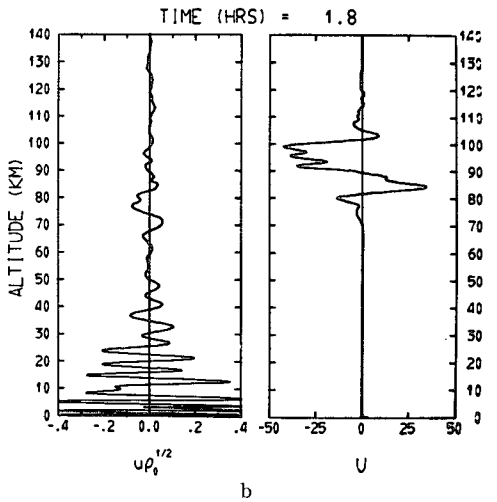

FIG. 2. Density-weighted horizontal wave velocity $u\rho_0^{\frac{1}{2}}$ and mean flow velocity U as functions of height at: a) 1.1, b) 1.8, c) 2.5, and d) 3.2 hr after initiation of continuous forcing. Random forcing generates waves of varying frequency and 15-km wavelength. Velocities are in m sec^{-1}.

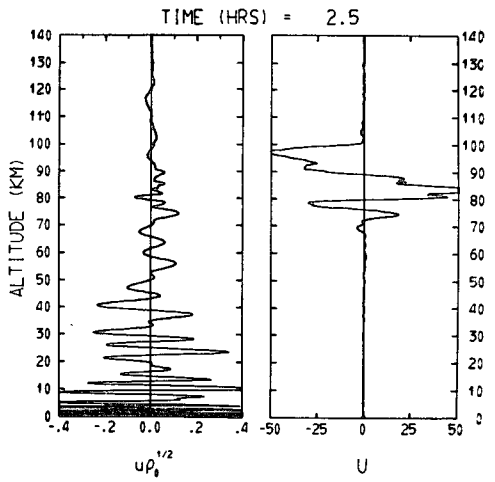

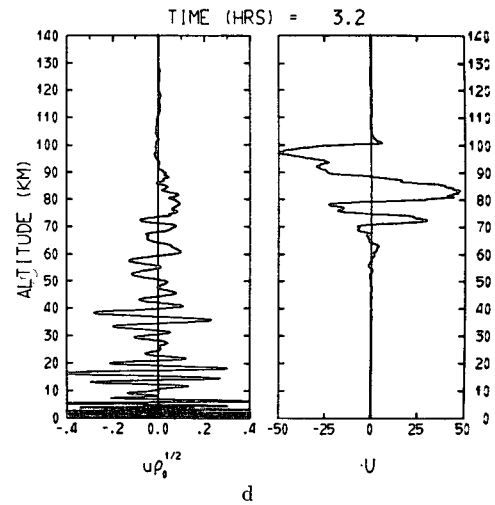

FIG. 2. (*continued*).

at lower levels; since the atmosphere is more dense at these levels, their development proceeds more slowly.

4. Conclusions

The conclusions we can reach from these numerical experiments must be carefully tempered by the limitations of the model. We have already mentioned the model's inability to reproduce instability and energy cascade into higher horizontal wavenumbers.

A potentially more significant limitation arises from the use of a single wavenumber. In effect, we assume a wave source that is horizontally periodic from minus to plus infinity. A more localized source would inject momentum into the "mean" flow in a horizontally limited region. This would allow horizontal pressure gradients to be developed to oppose changes in mean flow velocity. The mean flow momentum we inject with the wave could be advected away or even transmitted away as a large-scale wave. In a laboratory experiment, it can be transmitted out through the walls by pressure

differential. In general, then we will have overestimated the "local" changes in "mean" flow.

With these limitations in mind, we draw the following conclusions:

1) The momentum carried by the wave has produced substantial modification of the mean flow by the time a wave reaches a height at which it will break through instability. These changes in mean flow modify the character of the wave and of the breaking process. Any detailed analysis of wave breaking that does not take into account the interaction with mean flow must be suspect.

2) An appreciable fraction of wave energy is converted directly into mean flow kinetic energy. This conversion is much more efficient than driving large-scale circulations by heating derived from wave dissipation; the latter process can work with the thermodynamic efficiency of a Carnot cycle at best.

3) Fig. 2d shows a qualitative resemblance to upper atmosphere wind soundings. It has long been a question as to what fraction of these soundings is tidal and what fraction is internal gravity wave in nature. To do this we must add the question: What fraction is remnant mean wind momentum deposited by internal gravity waves? We note that the gravity waves that have produced the changes in mean wind in Fig. 2 have horizontal velocity amplitudes of only about 1 m sec^{-1} at 20 km.

A 16-mm film sequence of the two runs discussed here may be borrowed or purchased from the Computing Facility of the National Center for Atmospheric Research.

APPENDIX

Modeling of Eddy Viscosity in the Numerical Model

Eddy viscosity of Laplacian form is incorporated into the numerical model to simulate effects of eddy motions expected in regions of large velocity shear and to control the fine vertical structure that can otherwise reach unrealistic amplitudes in the nonlinear model. The model is unable to properly resolve the fine vertical structure, and unrealistic oscillations or exponential growth in time may result if this scale of motion reaches sufficient amplitude.

Eddy effects are modeled for both the mean flow and the horizontal component of the wave motions. In particular, $\nu\,\partial^2 U/\partial z^2$ is added to the equation of motion for the mean flow and $\nu\,\partial^2 u/\partial z^2$ to the equation of motion for the horizontal component of the wave motions, where ν is the kinematic coefficient of eddy viscosity, U the mean motion, u the horizontal component of wave motion, and z the vertical coordinate. Eddy viscosity effects dependent on horizontal derivatives are not included. Also neglected are all eddy diffusion effects on the vertical motion and the other dependent variables of the model. It is assumed that the scale height for variations in the mean density is larger than the vertical scale for velocity variations, so that $\nu\,\partial^2 u/\partial z^2$ can be replaced directly by $\nu\,\partial^2 \hat{u}/\partial z^2$ in the transformed wave equations used in this model where $\hat{u}$ is the density-weighted field variable for the horizontal component of wave velocity.

The standard centered three-point formula is used for the finite-difference formulation of the second derivative. Time differencing is forward with respect to the diffusion term so there is no difficulty defining all of the terms in the finite-difference equations. Numerical stability requires that $\nu\Delta t/(\Delta z)^2 \leqslant \frac{1}{4}$ where Δt is the time step and Δz the vertical grid increment. In the calculations presented in this paper, $\Delta t = 0.75$ sec and $\Delta z = 250$ m, giving a maximum allowable value of 2.08×10^4 m^2 sec^{-1} or several orders of magnitude larger than any values used.

Special boundary formulations are avoided by setting $\nu = 0$ at the lowest grid points for u and U. The magnitude of ν for the U calculations increases upward according to $\nu(z) = \nu_m[1 - e^{-z/20}]$, where ν_m is the maximum value of ν and z is the height in kilometers. The values of 100 m^2 sec^{-1} and 20 m^2 sec^{-1} for eddy viscosity referred to in the main text were the prescribed values for ν_m. The variables u and U are defined at different levels. The magnitude of ν used in the u calculations is set equal to that used for the U calculations half a grid space lower. At the upper boundary, the time changes due to this eddy viscosity are assumed to be equal to those one grid point below where explicit calculations can be made. This preserves the condition that u and U each have the same value at the upper two grid points.

Incorporation of the eddy viscosity finite-difference terms into the algorithm used for numerical calculations is made with no added difficulty according to the procedure described in Houghton and Jones (1969) and Jones and Houghton (1971).

Acknowledgments. Roger Breeding has provided a great deal of useful comment and stimulation. The numerical computations were handled by Sandra Fuller, whose talents in graphical output are greatly appreciated.

REFERENCES

Booker, J. R., and F. P. Bretherton, 1967: The critical layer for internal gravity waves in a shear flow. *J. Fluid Mech.*, **27**, 513–539.

Bretherton, F. P., 1969a: Momentum transport by gravity waves. *Quart. J. Roy. Meteor. Soc.*, **95**, 213–243.

——, 1969b: On the mean motion induced by internal gravity waves. *J. Fluid Mech.*, **36**, 785–803.

Einaudi, F., 1969: Singular perturbation analysis of acoustic-gravity waves. *Phys Fluids*, **12**, 752–756.

Hines, C. O., 1963: The upper atmosphere in motion. *Quart. J. Roy. Meteor. Soc.*, **89**, 1–42.

Hodges, R. R., 1967: Generation of turbulence in the upper atmosphere by internal gravity waves. *J. Geophys. Res.*, **72**, 3455–3458.

Houghton, D. D., and W. L. Jones, 1969: A numerical model for linearized gravity and acoustic waves. *J. Comput. Phys.*, **3**, 339–357.

Jones, W. L., 1971: The energy-momentum tensor for linearized waves in material media. *Rev. Geophys. Space Phys.*, **9**, 917–952.

——, and D. D. Houghton, 1971: The coupling of momentum between internal gravity waves and mean flow: A numerical study. *J. Atmos. Sci.*, **28**, 604–608.

Lindzen, R. S., 1968: The application of classical atmospheric tidal theory. *Proc. Roy. Soc. London*, **A303**, 299–316.

——, and J. R. Holton, 1968: A theory of the quasi-biennial oscillation. *J. Atmos. Sci.*, **25**, 1095–1107.

Matsuno, T., 1971: A dynamical model of the stratospheric sudden warming. *J. Atmos. Sci.*, **28**, 1479–1494.

Orlanski, I., and K. Bryan, 1969: Formation of the thermocline step structure by large amplitude internal gravity waves. *J. Geophys. Res.*, **74**, 6975–6983.